Comparison of the neutron halos for 4 different x-y aspect ratios, for momenta above 750 MeV/c

Jaap Doornbos, TRIUMF

February 14, 2003

Abstract

Results are given for four different aspect ratios. The collimator systems have been designed similarly to the system of Poblaguev's model 5. The contributions of individual collimators have been calculated. Absolute final intensities are determined. Contour plots are given at 14 m and 9.5 m from the target.

1 Introduction and summary

Calculations were done with GEANT FLUKA for four different x-y aspect ratios. The final beam size is the sum of the contributions of the individual collimators. An early collimator sees a small solid angle of acceptance towards the aperture of the last collimator. This limits the possible extent of the beam for neutrons which have a last scattering in that collimator. For a collimator downstream the solid angle will be larger, so that particles with a last scattering in that collimator will be more spread out. On the other hand, the chance of scattering from a collimator decreases for more downstream collimators. In this report the contributions of the individual collimators to the final beam size are determined, and then summed. 50 Million neutrons were generated and pursued through the collimator system. The coordinates and momenta of those neutrons that reached 14 m, were collected in a file which was later analyzed. In order to keep the length of the file manageable, the accumulation of data for those neutrons that came directly from the target without any further scattering was stopped after 625,000 neutrons were processed. Those results were then later multiplied by a factor 80. Similarly, the accumulation for neutrons that only scattered in the spoiler was stopped after 12,500,000 neutrons were processed. The results were later multiplied by a factor 4.

In section 2 the construction of the collimator systems is discussed. See figures 1 to 3. On the basis of the layout it is possible to obtain geometric limits on the beam size, in section 3. More realistically, scatter plots of the contributions of individual collimators to the final beam size are shown in section 4. The fractional contributions of the individual collimators are discussed in section 5. The conclusion is that the scattering on the individual collimators increases by a factor 3 when the vertical acceptance angle is increased from ± 2.0 mr to ± 3.8 mr. The beam also becomes much wider in the vertical plane. Section 6 shows that the contribution of inelastic scattering in each collimator increases the more downstream it is.

Intensity distributions projected on the x and y axes are given in section 7.1 in relative terms. Absolute intensities are determined in section 7.2. The original KOPIO proposal gives on page 141, in table 4, the neutron yield above 100 MeV as $1.04\ 10^{-6}$ per proton per μsr. Although this report considers only neutrons above 750 MeV/c or 262 MeV, this is the number used here. Assuming 10^{14} protons per pulse and 500 μsr, and taking into account that half of all neutrons are lost in the 7 cm thick Lead spoiler, the total number of accepted neutrons is $25\ 10^{9}$. The central luminosity is 25 million neutrons per cm^2. Figure 20 shows intensity contours at 14 m. The 0.02 percent contour corresponds to 5,000 neutrons per cm^2.

Figure 21 shows the intensity contours at 9.5 m. In this case the 0.02 percent contour corresponds to 11,000 neutrons per cm^2.

2 Construction of collimator system

The collimator system has been designed similar to the standard system of Poblaguev's model 5. That model has a vertical angle acceptance of ± 2.6 mr, and a horizontal angle acceptance of ± 48 mr. It was modified slightly, and the collimator systems for other aspect ratio's were then constructed in a similar way, so that a systematic and consistent comparison becomes possible. The following four cases are compared.

1. Vertical acceptance $\pm$ 2.6 mr, and horizontal acceptance of ± 51 mr.
2. Vertical acceptance $\pm$ 3.2 mr, and horizontal acceptance of ± 42 mr.
3. Vertical acceptance $\pm$ 3.8 mr, and horizontal acceptance of ± 35 mr.
4. Vertical acceptance $\pm$ 2.0 mr, and horizontal acceptance of ± 66 mr.

Cases 1 to 3 have progressively larger vertical acceptance, and smaller horizontal acceptance. It is interesting to also go in the opposite direction by decreasing the vertical acceptance. This is case 4. The collimator apertures are listed in tables 1 and 2 The first 3 figures show how the collimator apertures are determined. Figure 1 shows the whole vertical collimator, and figure 2 shows the beginning. Figure 3 shows the horizontal collimators. These figures are for case 1, namely 2.6 mr by 51 mr acceptance. The 7 cm thick lead spoiler is located 50 cm from the 10 cm long production target. The beam takes off at 45 degrees. The vertical proton spot on the target has a full width of 2 mm. The horizontal size, projected at right angle to the kaon beam direction, is taken as ± 4 cm for the purpose of constructing the apertures.

The construction starts in figure 2.

- The blue line from the center of the production target has a divergence of 2.6 mr. This determines the aperture of 2.6 mm at the entrance of collimator C0, which starts at 1 m. The slope of C0 is also 2.6 mr. At the exit of C0 the aperture is 5.2 mr.

- The red line starts 1 mm from the axis. This is half the vertical source size. It is connected with the 5.2 mm aperture at the entrance of C1 to determine the slope angle of C1. The line is extended to z=3.5 m, which is the start of C2.

- The width of the spoiler just covers the aperture of the first collimator. It is determined by drawing a line from 1 mm above the axis at z=0 to +2.6 mm at z=1.0 m, and then interpolating. The green line connects the extreme point of the spoiler with the entrance aperture of C2. It determines the slope of C2. After extension to z=5.0 m it gives the entrance aperture of C3.

- The rest of the collimator is shown in figure 1. The red line connects the exit aperture of C0 with the entrance aperture of C3, and determines the slope of C3. It is extended to z=6.5 m to give the entrance aperture of C4.

- The blue line connects the exit of C1 with the entrance of C4.

The horizontal collimator is designed as follows in figure 3.

- A first blue line has a divergence of 51 mr. This is 3 mr more than in the standard model 5. The reason is that the slope of the collimators is smaller. In order to maintain the acceptance for the whole horizontal source size the initial divergence has to be larger. The blue line gives the slope of C1, and after extension to z=3.5 m, determines the entrance aperture of C2.

- The red line starts 4 cm from the axis at z=0 and connects with the entrance aperture of C2. It determines the slope of C2 and C3 and the entrance aperture of C4.
- The second blue line connects the entrance aperture of C1 with the entrance aperture of C4, and determines the slope of C4.

The same procedure was used to construct the collimator systems for the other 3 cases.

3 Preliminary limits on the beam size at 14 m

Tables 1 and 2 make it possible to obtain geometric limits on the beam size at 14 m, by determining the maximum acceptance of the collimator system from a given point along the beam. They are shown in figure 4. For instance, the inner blue line indicates the maximum size of the beam for those neutrons that come directly from the production target, without intersecting any collimator. The inner red line indicates the maximum beam size that is possible for neutrons that have scattered in the spoiler, but do not intersect the collimators. The green line gives the maximum beam size for particles scattered before the exit of C0 and no further intersecting of the other collimators. The next red line shows the maximum size for neutrons that have their last scattering before the exit of C1. The next blue and red lines are similar for the exits of C2 and C3.

The beam size is quite restricted vertically for neutrons that scatter before the exit of C2. Even scattering in C3 constrains the beam vertically to 15 cm from the axis for the 2.0 mr case, up to 28 cm for the 3.8 mr case. Only if the scattering takes place in C4(not shown here) will the vertical size be large.

It is expected that the horizontal limits are less important. They have been arrived at by drawing lines from the aperture of one collimator at one side of the axis to an other aperture of an other collimator on the other side of the axis. If the vertical angle of a neutron is only moderately large it will already be scattered on the top or bottom of a collimator, and not on the side. Therefore, crossing from one side to the opposing side is fairly unlikely.

The importance of the contribution to the beam tail from scattering in the various collimators depends, of course on the amount of beam that is scattered. This is the subject of the section 5.

4 The beam tail from individual collimators

The limits obtained in the previous sections are extremes. Therefore scatter plots at 14 m show more realistic results from Monte Carlo calculations for the 2.6 mr case. Figure 5 is for neutrons which have a last scattering in the spoiler, in C0 or in C1. The scattered points approach the boundaries given in figure 4, but the intensity of the distributions decreases near the boundaries. Figure 6 is also for the 2.6 mr case, but for collimators C2 to C4. This figure shows an additional feature. Namely, the green points are elastically scattered neutrons and the blue points are inelastic neutrons. There is again reasonable agreement vertically for C2 and C3 with the boundaries of figure 4. The tendency is for the inelastic neutrons to be more from the axis on average than the elastic neutrons. This becomes overwhelmingly clear in the bottom plot for neutrons that have a final scattering in collimator C4. It is mostly the inelastic scattering in C4 that is responsible for a diffuse background of neutrons throughout the whole back face of the decay volume at 14 m. Unless a way is found to restrict the fraction that is scattered in C4, there is no way to limit this background.

Figures 7 to 9 show the scatter plots from C2, C3 and C4 for the other 3 cases. The bottom plots show clearly that the number of particles scattered in C4 increases with vertical acceptance angle.

For the 2.6 mr case the distributions projected on x and y axis are given in figures 10 to 13. They have been arbitrarily normalized to 100 events per bin for neutrons coming directly from the production target. This has been done to facilitate a comparison between the contributions of the various collimators.

5 Fractional contributions from the collimators

Table 3 shows the fraction of beam scattered at the latest in the indicated collimators. The first row shows that 95 to 97 percent of the final beam comes directly from the production target without further scattering. About 2.5 percent comes from neutrons with a last scattering in the spoiler for the 2.0 mr case. This fraction increases as the vertical acceptance angle increases. The contributions from last scatterings in the following collimators become progressively less but are spread out over a wider area at 14 m.. In all cases the fraction becomes larger when the vertical acceptance increases. The fractions are plotted in figure 14. On the horizontal axis the number -2 indicates the production target, and the number -1 the spoiler. The other numbers indicate collimators C0 to C4. A more detailed comparison of the various cases is given in figure 15 for collimators C1 to C4. Here the horizontal axis indicates the vertical acceptance angle for the 4 cases. It is 2.0 mr for case 4, 2.6 mr for case 1, 3.2 mr for case 2 and 3.8 mr for case 3. In order to compare the results for the different collimators, the data of table 3 have been arbitrarily normalized to the number 10 for the fractions at 3.8 mr. Each plot has only 4 points, but the dependence on the acceptance angle is roughly linear. The solid line in all four plots is given by the equation

$$\text{fraction} = 3.86 * (\phi - 1.15) \tag{1}$$

Here ϕ is the vertical angle in mr. In other words the dependence on the vertical angle is approximately the same for all 4 collimators. The line does not go through 0 at $\phi = 0$, but there is an offset of 1.15 mr, probably due to the finite vertical target size of ± 1 mm, and the way the collimators apertures are determined. All fractions increase about a factor 3 between the 2.0 mr case and the 3.8 mr case.

6 The importance of inelastic scattering

The neutrons which reach 14 m after having the last scattering in the spoiler are for the most part elastically scattered neutrons, but there is a small number of about 6 percent that has inelastically scattered. The importance of inelastic scattering increases for neutrons that have a last scattering in C0, C1, and so on. The closer a collimator is to the decay volume the more important inelastic scattering becomes. The inelastic percentage is listed in table 4.

7 Total intensity distributions

7.1 Relative total distributions

The projected total intensity distributions were binned in 1 cm bins vertically and in 5 cm bins horizontally. They are shown in figures 16 and 17.

Figure 18 shows the same distributions normalized to 1.0 at x=0 and y=0. For instance, for case 1 the vertical intensity drops 4 decades at 9.6 cm.

Figure 19 shows the fraction of intensity outside the indicated vertical or horizontal area. For instance, in case 1 a fraction of 10^{-4} of the total intensity is outside y=9.0 cm.

Figure 20 shows intensity contours. The data are binned in an x-y grid, in steps of 1 cm in y and 5 cm in x. The intensity per 2-dimensional bin is within a few percent equal to 80,000 per bin in the central 5 bins, which cover an area of 1 cm y by 25 cm x. This corresponds to 16,000 per cm^2. But the quadrant shown has the results of all 4 quadrants, since the absolute values of x and y were taken. Therefore, actually there are 4,000 per cm^2 in the center bins. The total number of Monte Carlo events at 14 m turns out to be 4 Million.

7.2 Absolute intensities

According to table 4, page 141, of the proposal the neutron yield above 100 MeV is $1.04 * 10^{-6}$ per proton per μsr at 46.5 degrees. This report considers only neutrons above 750 MeV/c which is 262 MeV, but close enough. The acceptance of the collimator system is 500 μsr. Half is lost in the spoiler. If there are 10^{14} protons per pulse, then the total number of neutrons arriving at 14 m is $10^{14} * 1.04 * 10^{-6} * 500 * 0.5 = 25 * 10^{9}$. Therefore the 4 Million Monte Carlo events correspond to $25 * 10^{9}$ real neutrons, or 1 Monte Carlo event corresponds to 6,250 real neutrons.

In the center of the distribution there are 4,000 Monte Carlo events per cm^2, corresponding to 25 million real neutrons per cm^2. The 10 percent contour in figure 20 corresponds to 2.5 million neutrons per cm^2. The 1 percent contour corresponds to 250,000 real neutrons per cm^2. The 0.2 percent contour corresponds to 50,000 real neutrons per cm^2. The 0.02 percent contour corresponds to 5,000 real neutrons per cm^2. Beyond that it is not possible to make contour plots due to lack of statistics. This is clear from the scatter plots in figures 6 to 9.

Figure 21 shows the contour plots at 9.5 m. The data were binned in 0.4 cm bins vertically and 3.0 cm horizontally. The central luminosity is 55 million per cm^2. The 0.02 percent contour corresponds to 11,000 neutrons per cm^2.

8 Notes added in proof

1. The collimator material was Tungsten.

2. The yield above 100 MeV was used for the normalization. The yield above 262 MeV is probably a factor 2 lower.

Table 1: Horizontal apertures of collimators

case		2.0 mr	2.6 mr	3.2 mr	3.8 mr
	z (cm)	x (cm)	x (cm)	x (cm)	x (cm)
spoiler half width	50	6.3	5.55	5.10	4.75
COL0 in	100	200	200	200	200
COL0 out	200	200	200	200	200
COL1 in	200	13.2	10.2	8.4	7.0
COL1 out	300	19.8	15.3	12.6	10.5
COL2 in	350	23.1	17.85	14.7	12.25
COL2 out	450	30.9	24.09	20.1	16.95
COL3 in	500	34.8	27.21	22.8	19.3
COL3 out	600	42.6	33.45	28.2	24.0
COL4 in	650	46.5	36.57	30.9	26.35
COL4 out	850	73.1	57.37	48.5	41.35

Table 2: Vertical apertures of collimators

case		2.0 mr	2.6 mr	3.2 mr	3.8 mr
	z (cm)	y (mm)	y (mm)	y (mm)	y (mm)
spoiler half width	50	1.5	1.8	2.1	2.4
COL0 in	100	2.0	2.6	3.2	3.8
COL0 out	200	4.0	5.2	6.4	7.6
COL1 in	200	4.0	5.2	6.4	7.6
COL1 out	300	6.5	8.3	10.1	11.9
COL2 in	350	7.75	9.85	11.95	14.05
COL2 out	450	10.85	13.75	16.65	19.55
COL3 in	500	12.4	15.7	19.0	22.3
COL3 out	600	17.9	22.7	27.5	32.3
COL4 in	650	20.65	26.2	31.75	37.3
COL4 out	850	36.25	46.0	55.75	65.5

Table 3: Fraction of beam directly from target, or with last scattering in spoiler or indicated collimator.

case	2.0 mr	2.6 mr	3.2 mr	3.8 mr
target	0.96797	0.96267	0.95708	0.95089
spoiler	0.02535	0.02911	0.03298	0.03751
COL0	0.00536	0.00616	0.00707	0.00803
COL1	0.00108	0.00166	0.00228	0.00280
COL2	0.000218	0.000338	0.000498	0.000671
COL3	0.0000228	0.0000379	0.0000633	0.0000740
COL4	0.0000108	0.0000167	0.0000243	0.0000280

Table 4: Inelastic percentage of beam with last scattering in spoiler or in indicated collimator

case	2.0 mr	2.6 mr	3.2 mr	3.8 mr
target	0.0	0.0	0.0	0.0
spoiler	6.6	6.0	5.3	4.9
COL0	11.5	11.1	11.5	10.0
COL1	23.1	19.7	17.4	15.1
COL2	19.9	20.0	17.2	17.9
COL3	30.1	25.2	29.7	27.0
COL4	38.6	52.3	47.8	52.2

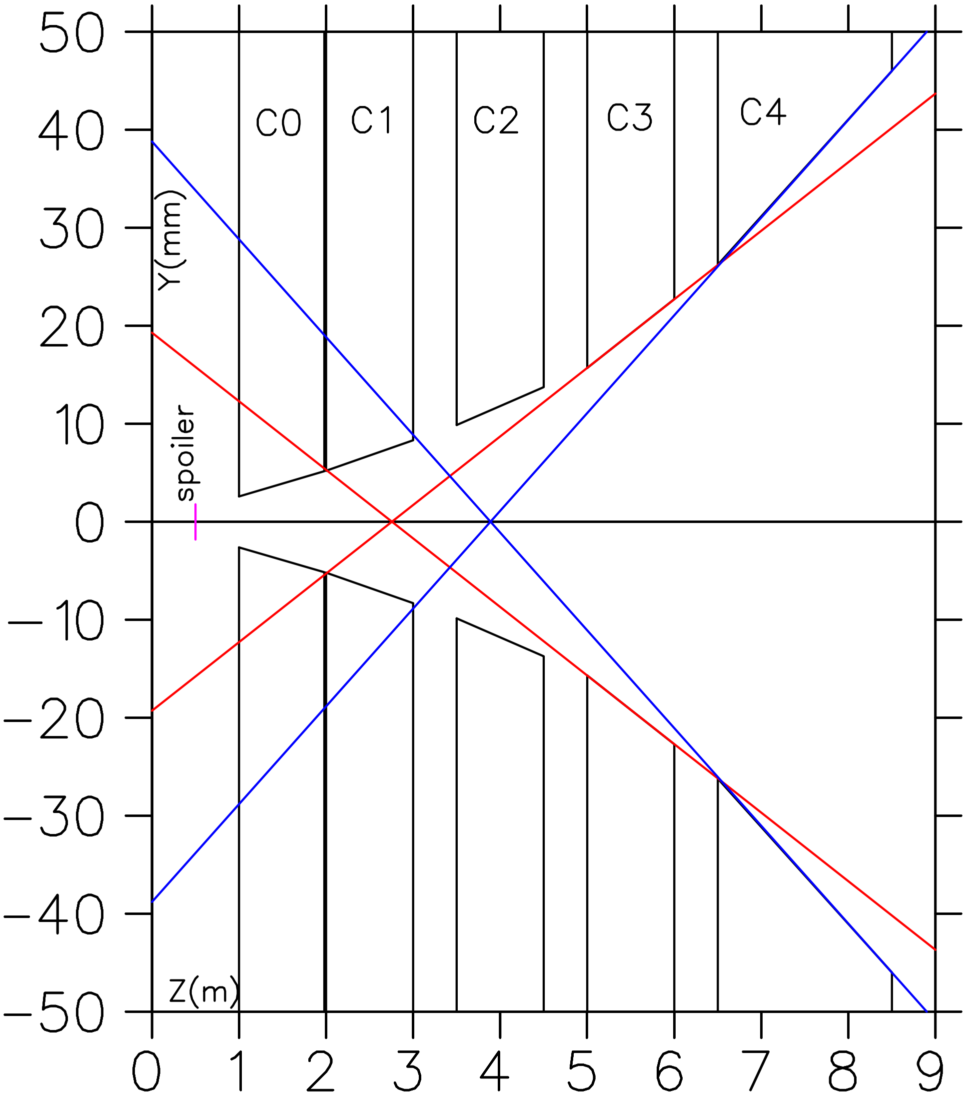

Figure 1: Construction of the vertical apertures of collimators C3 and C4

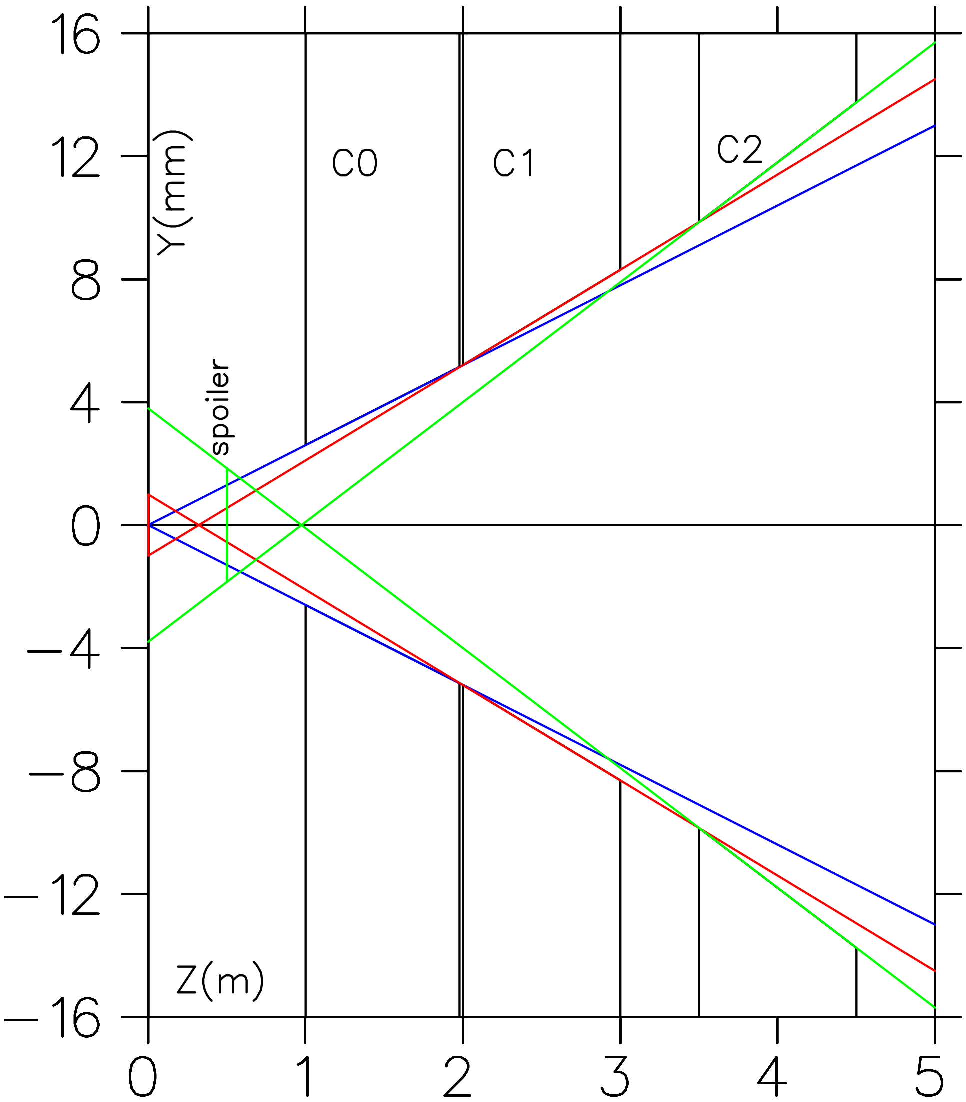

Figure 2: Construction of the vertical apertures of collimators C0 to C2

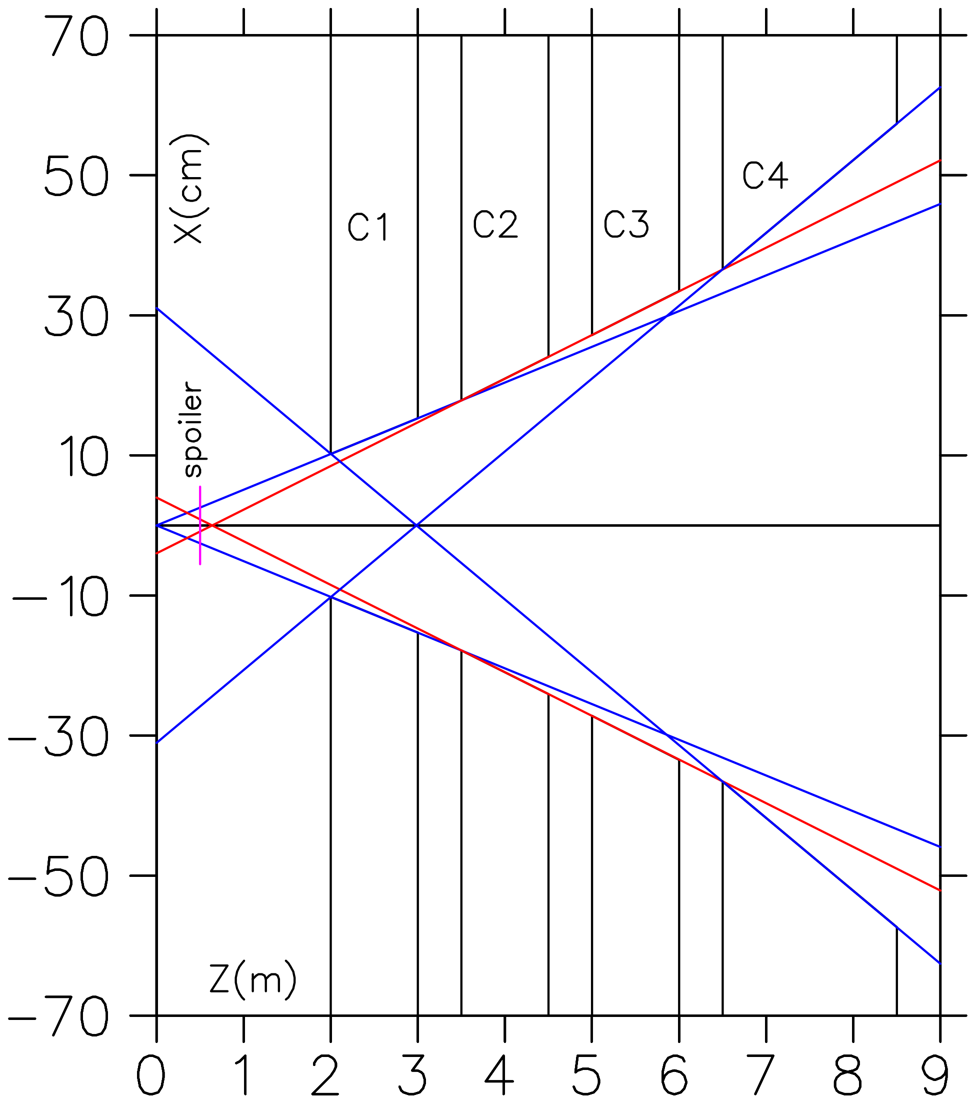

Figure 3: Construction of the horizontal apertures of the collimators

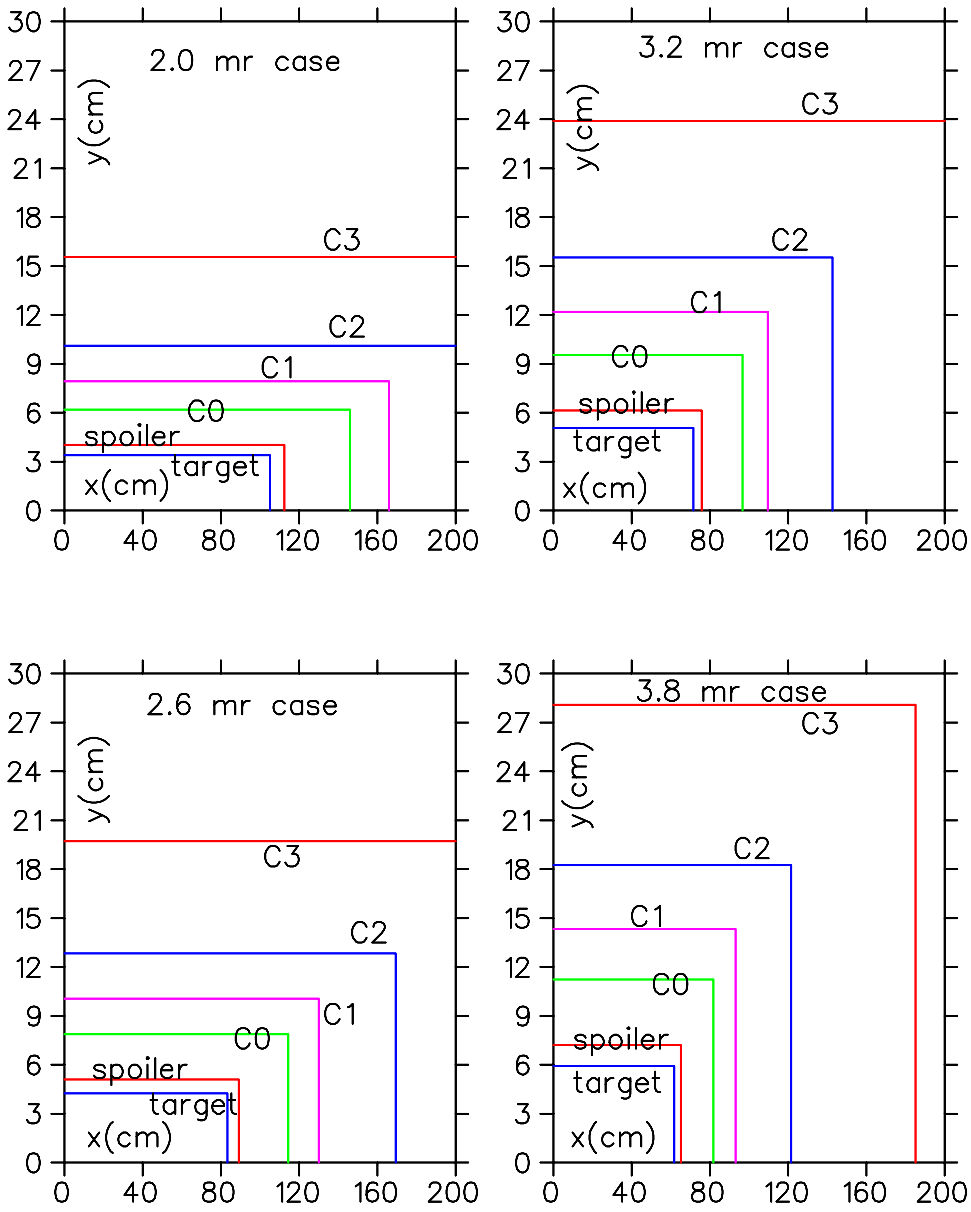

Figure 4: Limits to the final beam size on the basis of purely geometric considerations

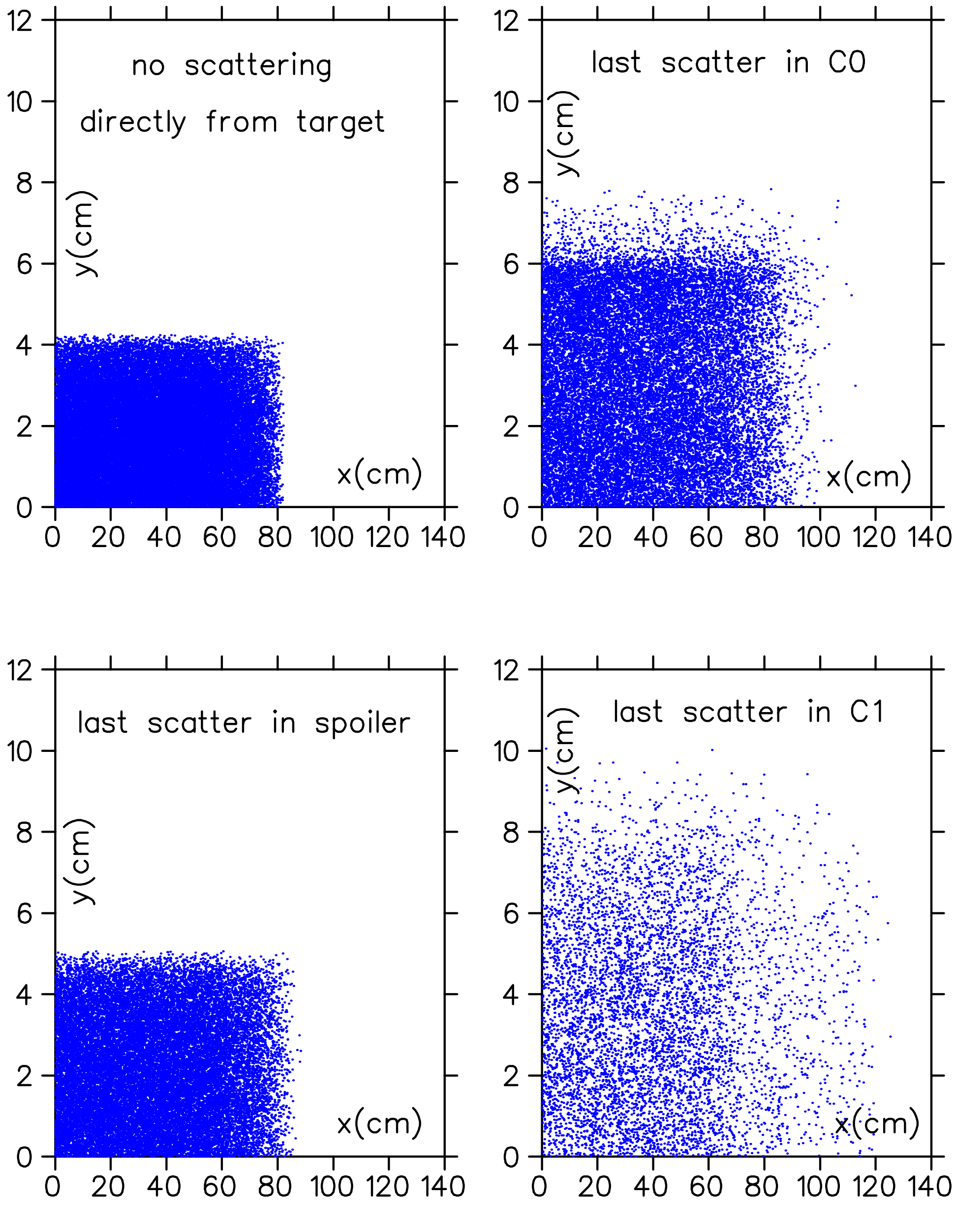

Figure 5: Four scatter plots at 14 m for the 2.6 mr case

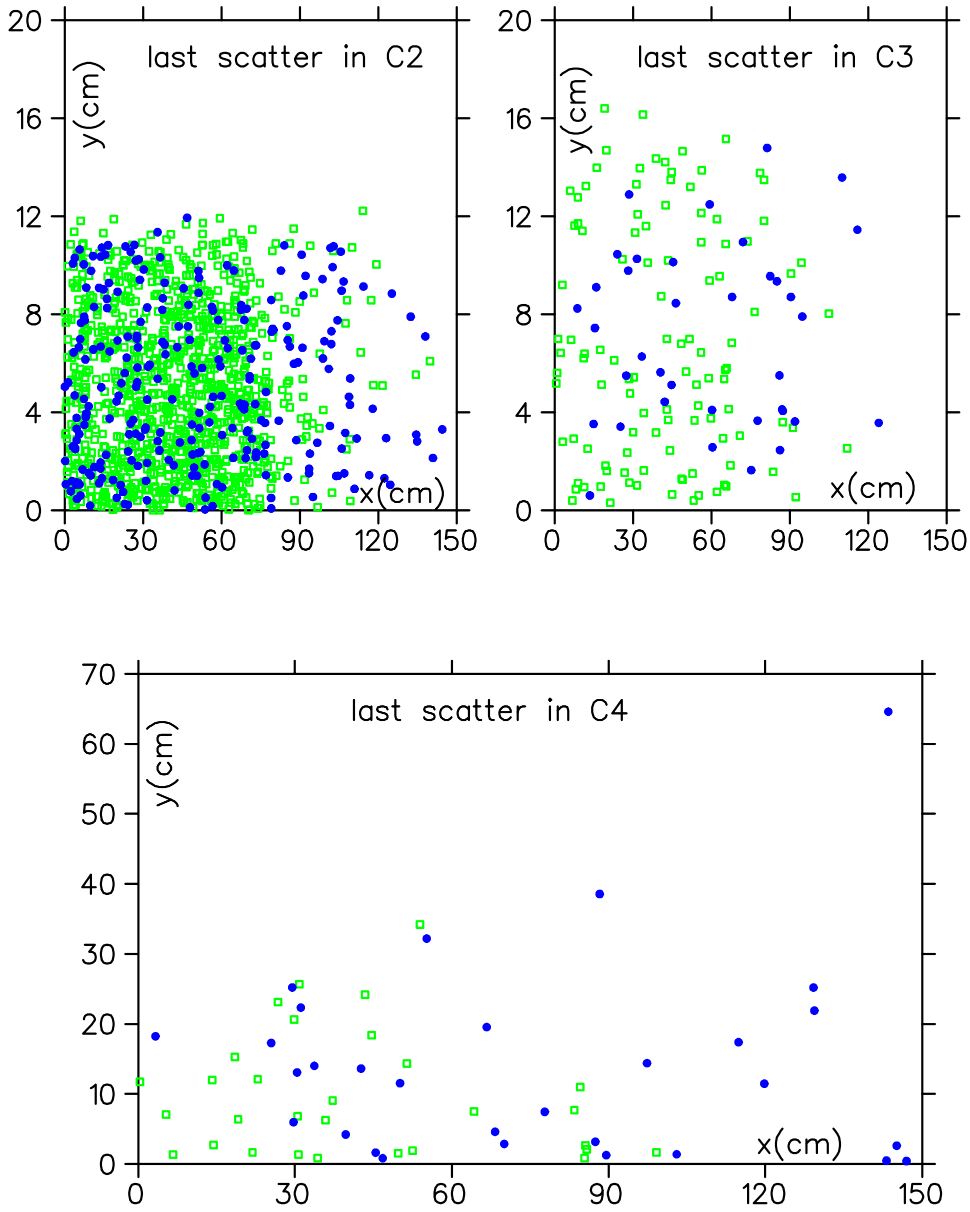

Figure 6: Scatter plots from collimators C2, C3 and C4 at 14 m for the 2.6 mr case

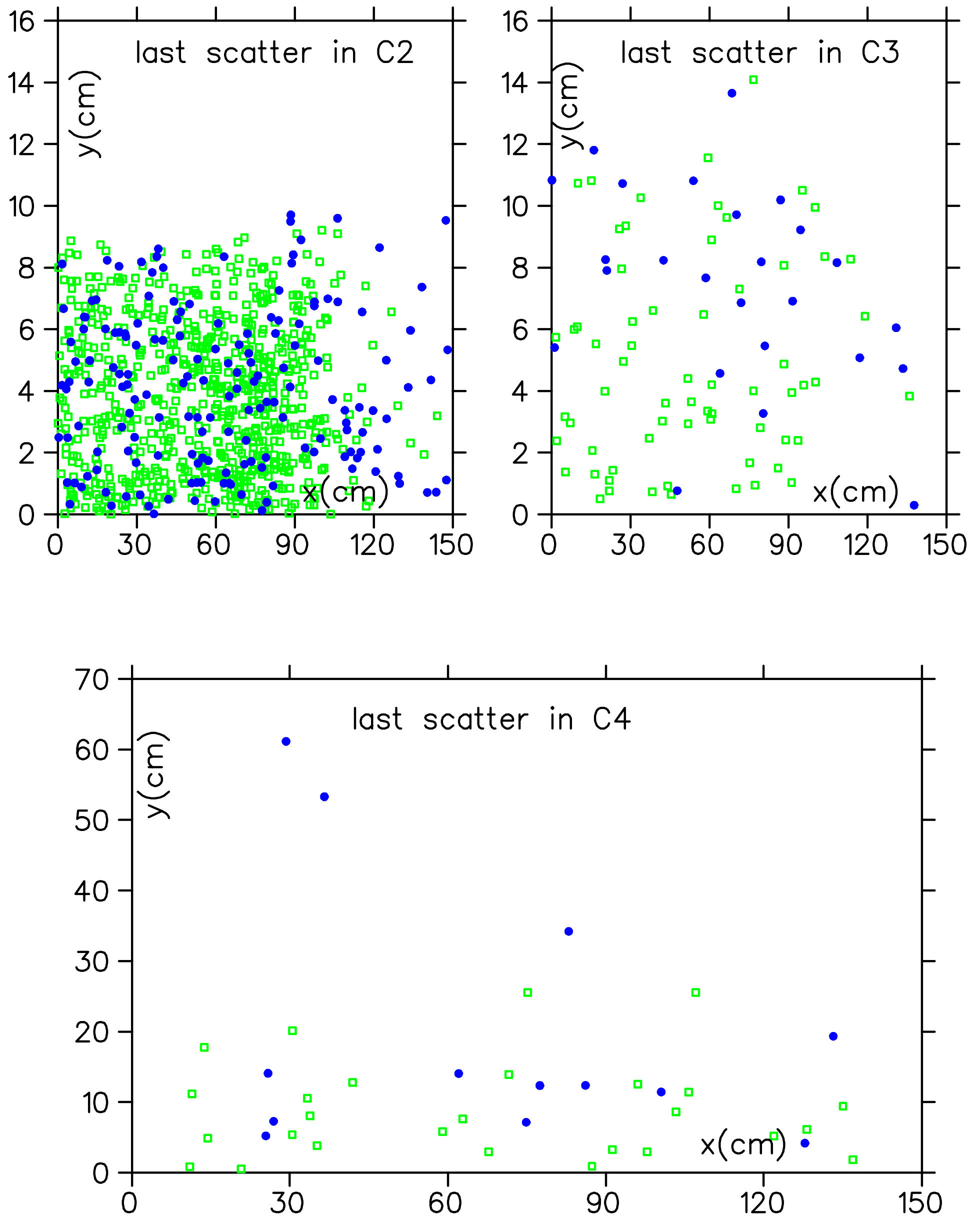

Figure 7: Scatter plots from collimators C2, C3 and C4 at 14 m for the 2.0 mr case

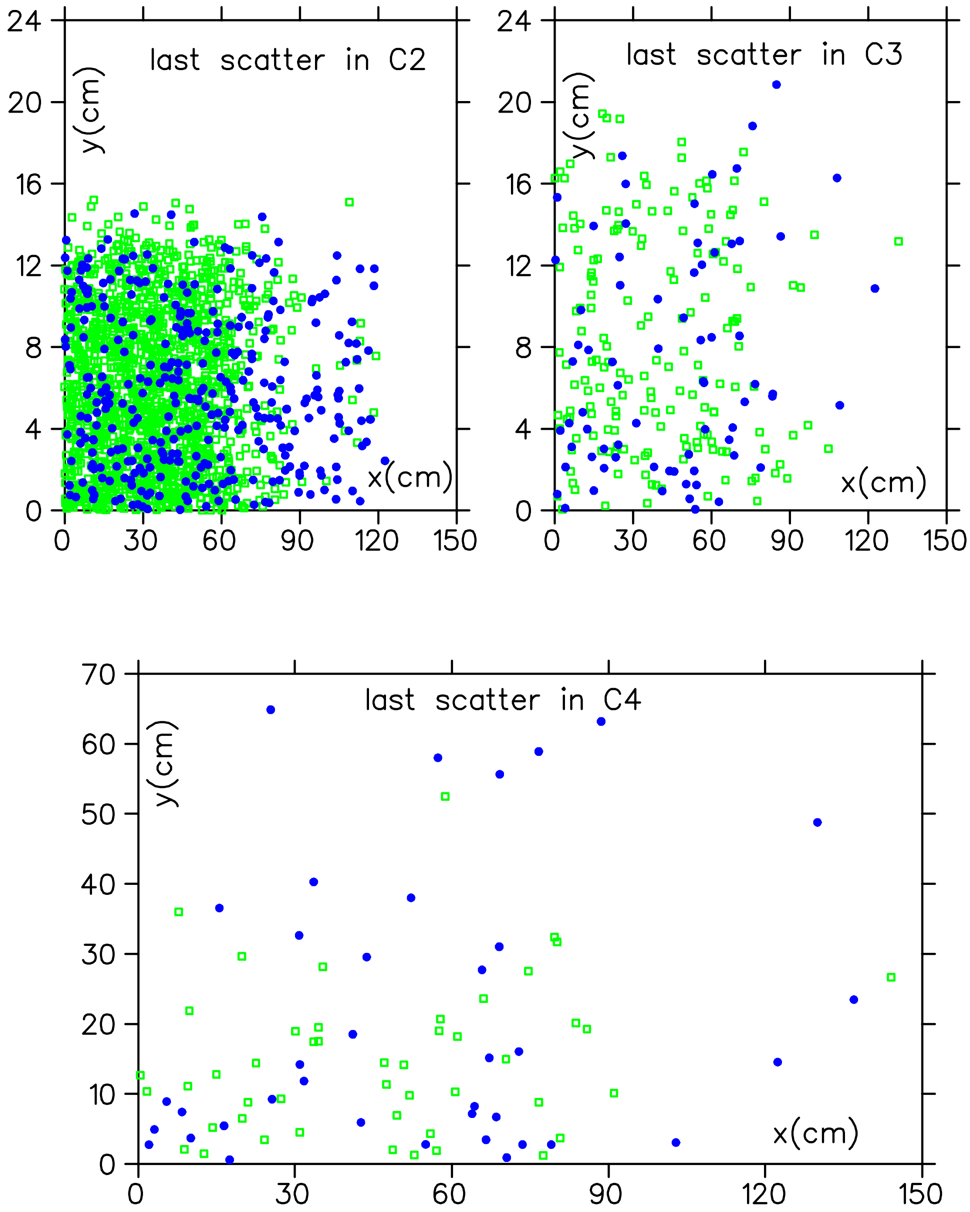

Figure 8: Scatter plots from collimators C2, C3 and C4 at 14 m for the 3.2 mr case

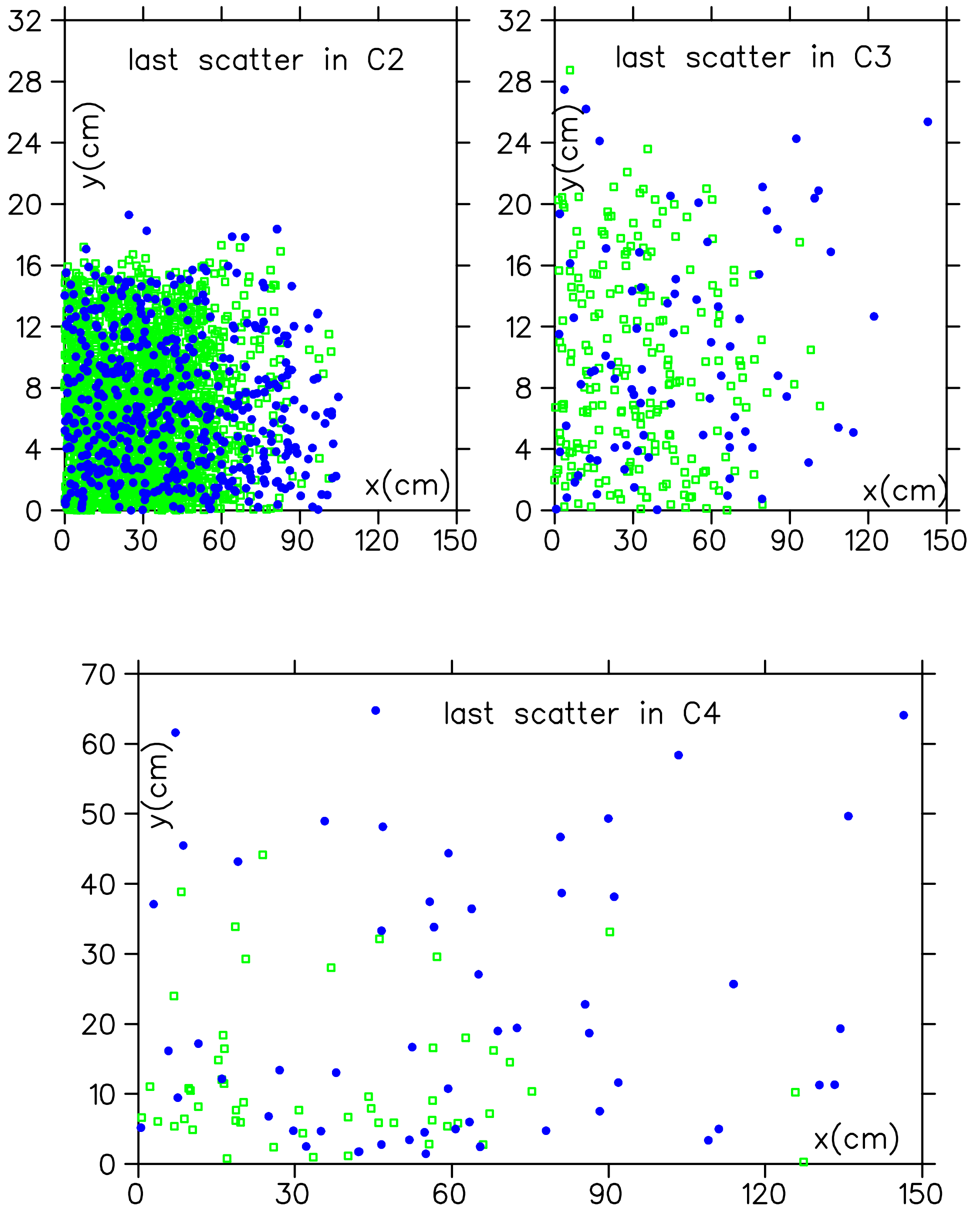

Figure 9: Scatter plots from collimators C2, C3 and C4 at 14 m for the 3.8 mr case

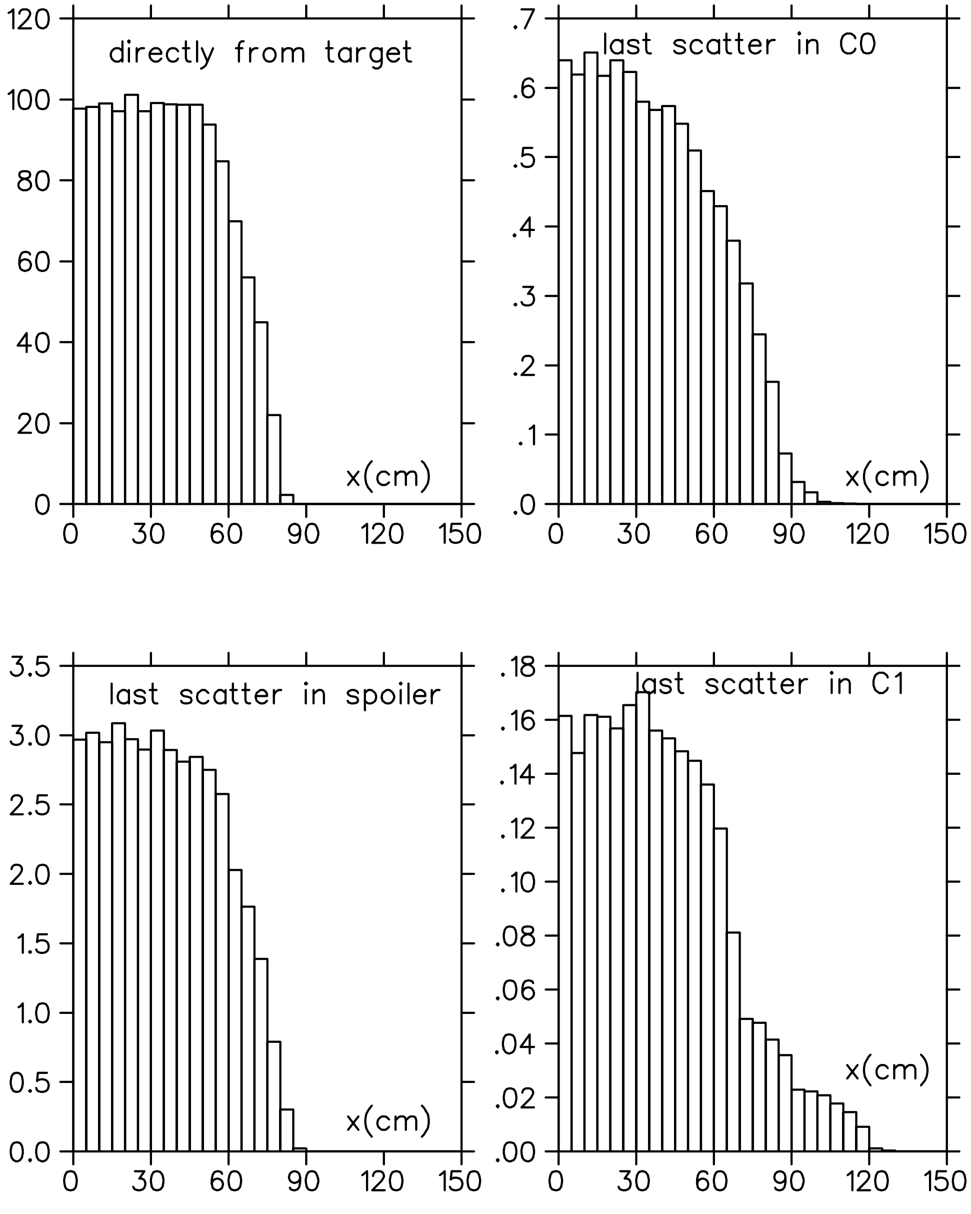

Figure 10: Projected horizontal distributions at 14 m for the 2.6 mr case

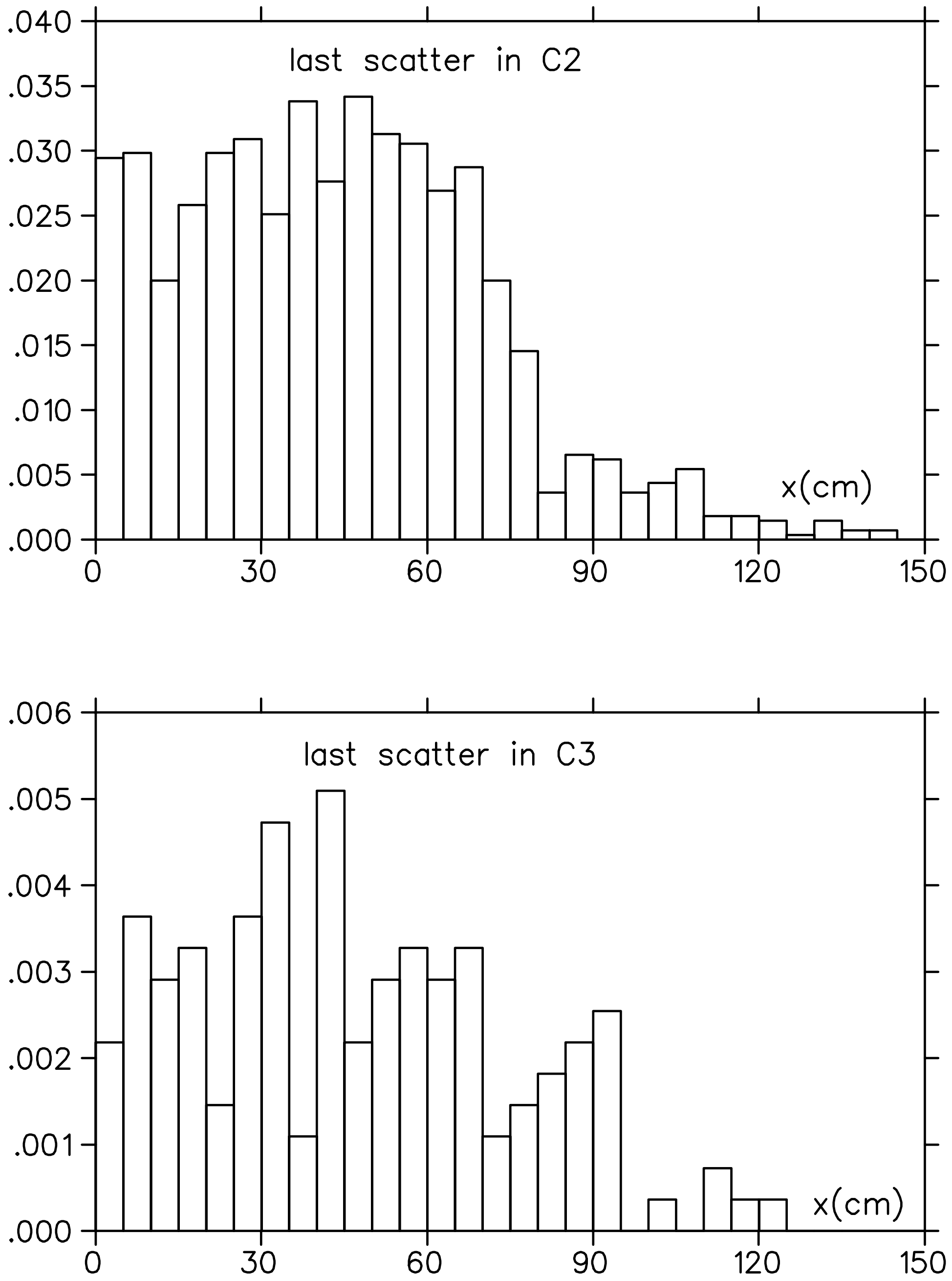

Figure 11: Two more projected horizontal distributions at 14 m for the 2.6 mr case

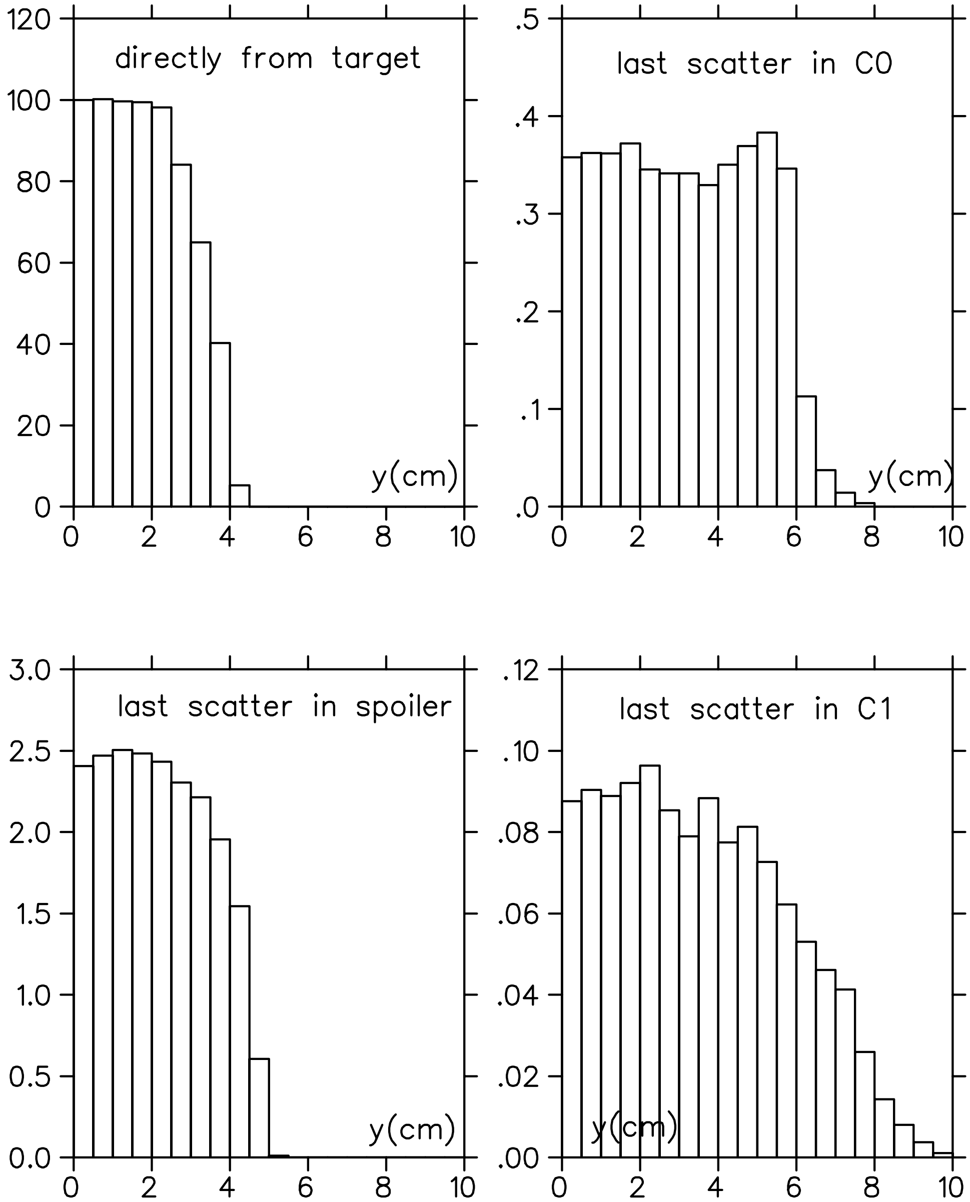

Figure 12: Projected vertical distributions at 14 m for the 2.6 mr case

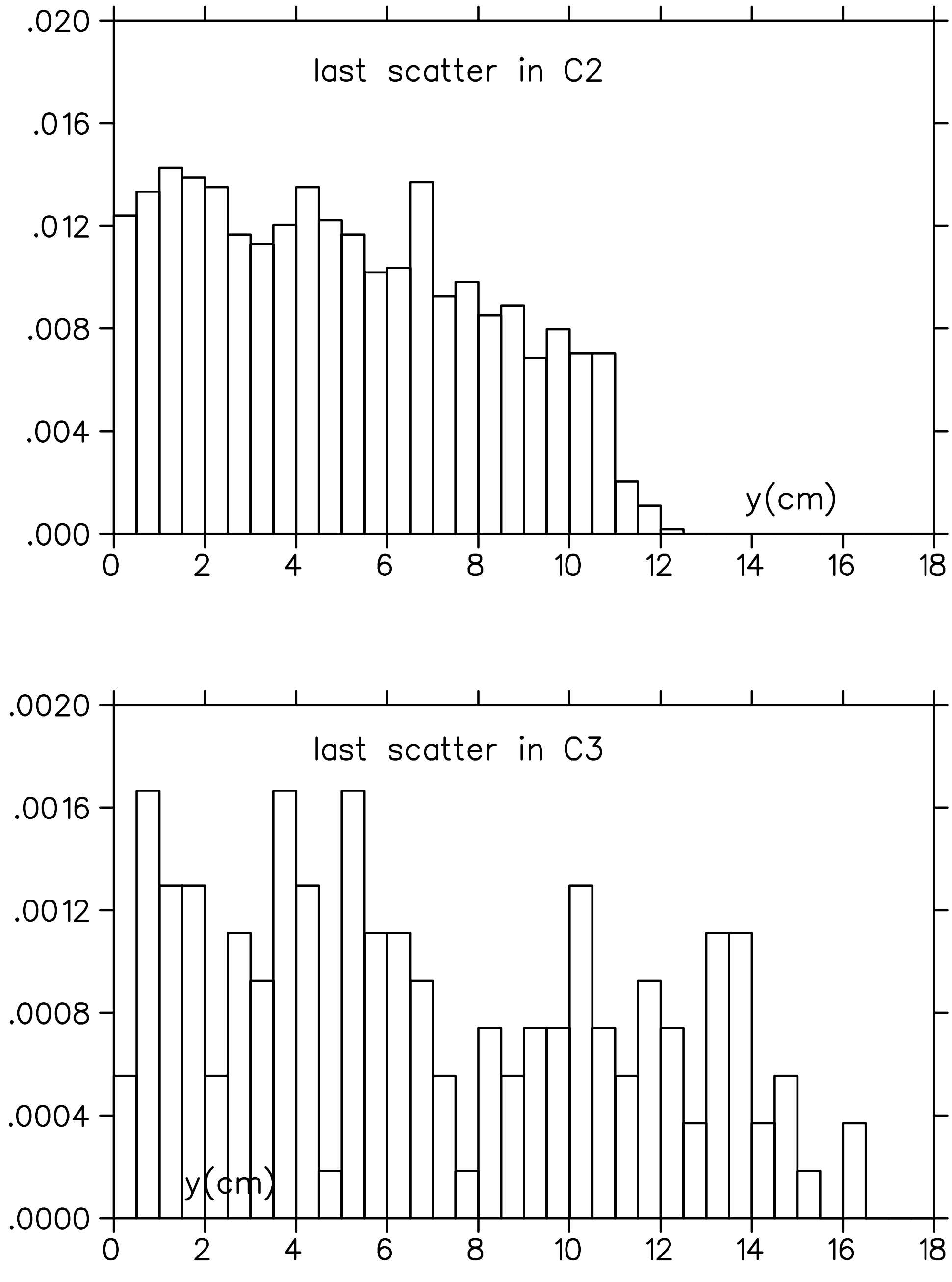

Figure 13: Two more projected vertical distributions at 14 m for the 2.6 mr case

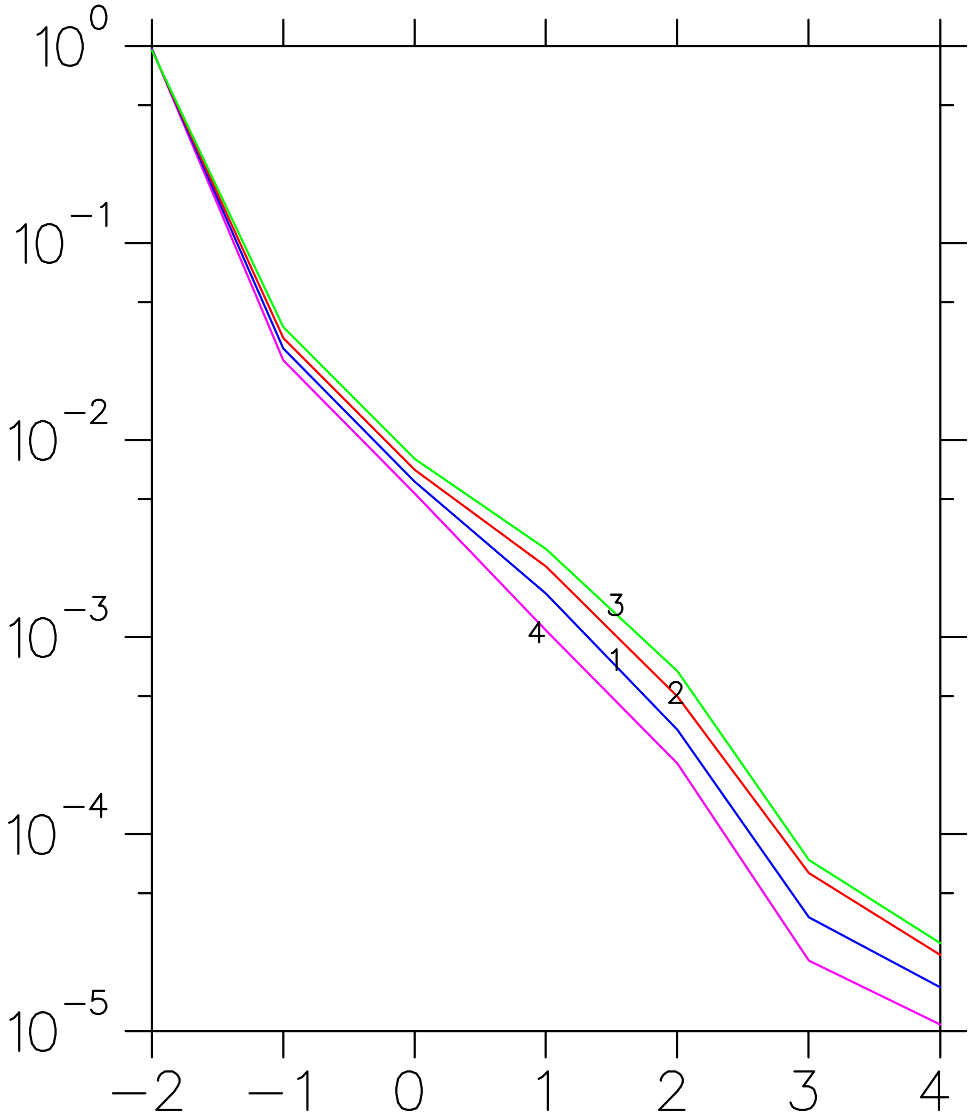

Figure 14: Fractions of neutrons, scattered lastly in the indicated collimators. See text for the meaning of the numbers on the horizontal axis

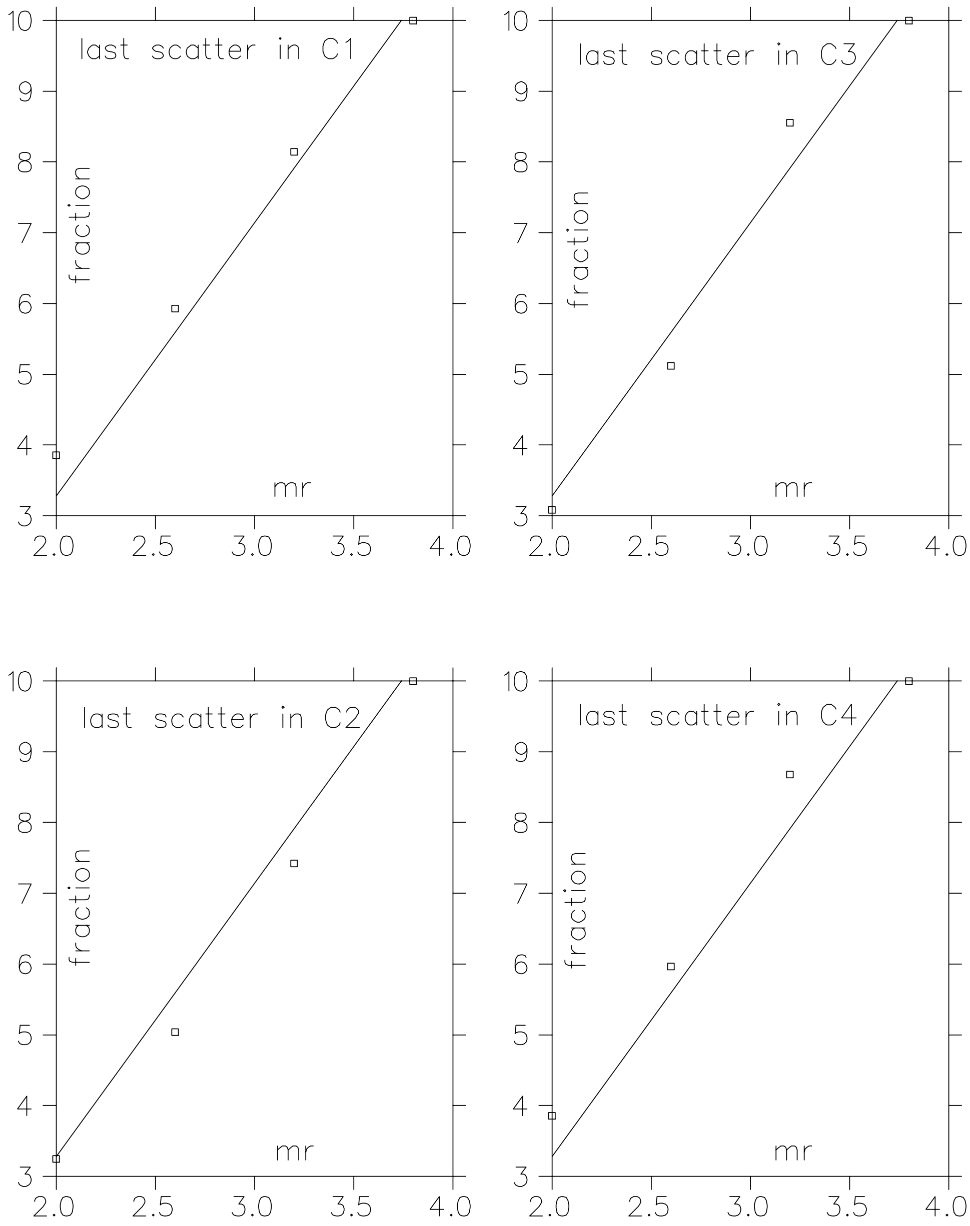

Figure 15: Normalized scatter fractions plotted against the vertical acceptance angle. See text for the meaning of the numbers on the horizontal axis

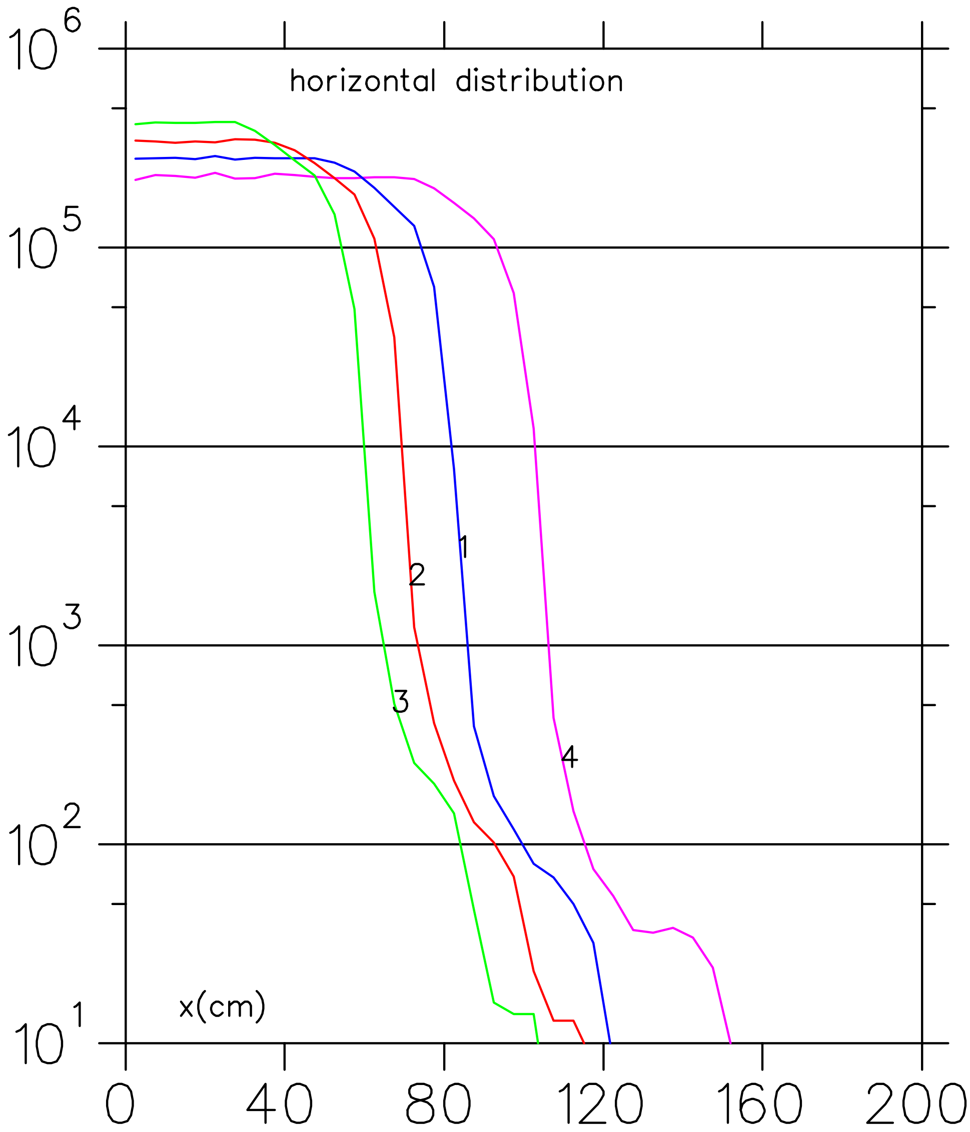

Figure 16: Horizontal beam profile at 14 m for all four cases

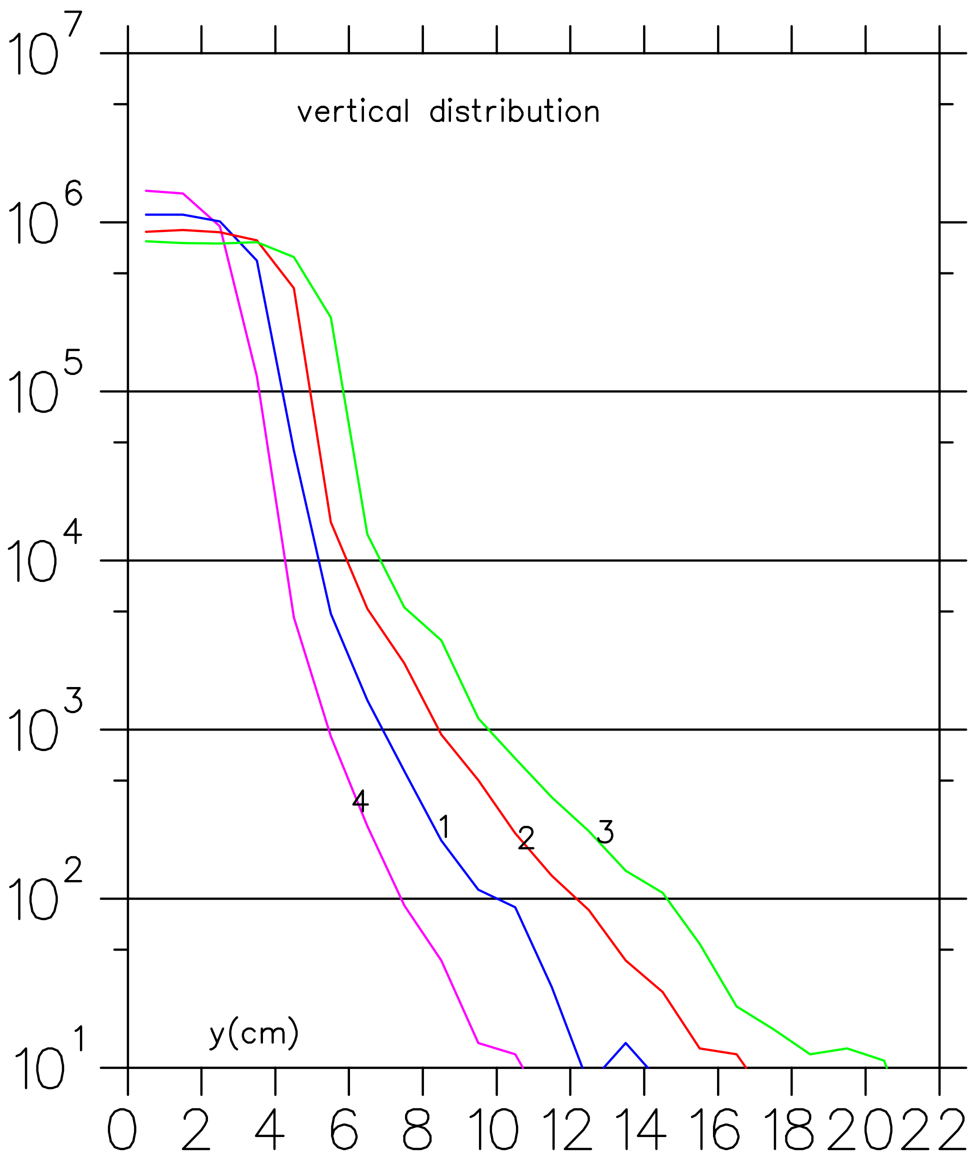

Figure 17: Vertical beam profile at 14 m for all four cases

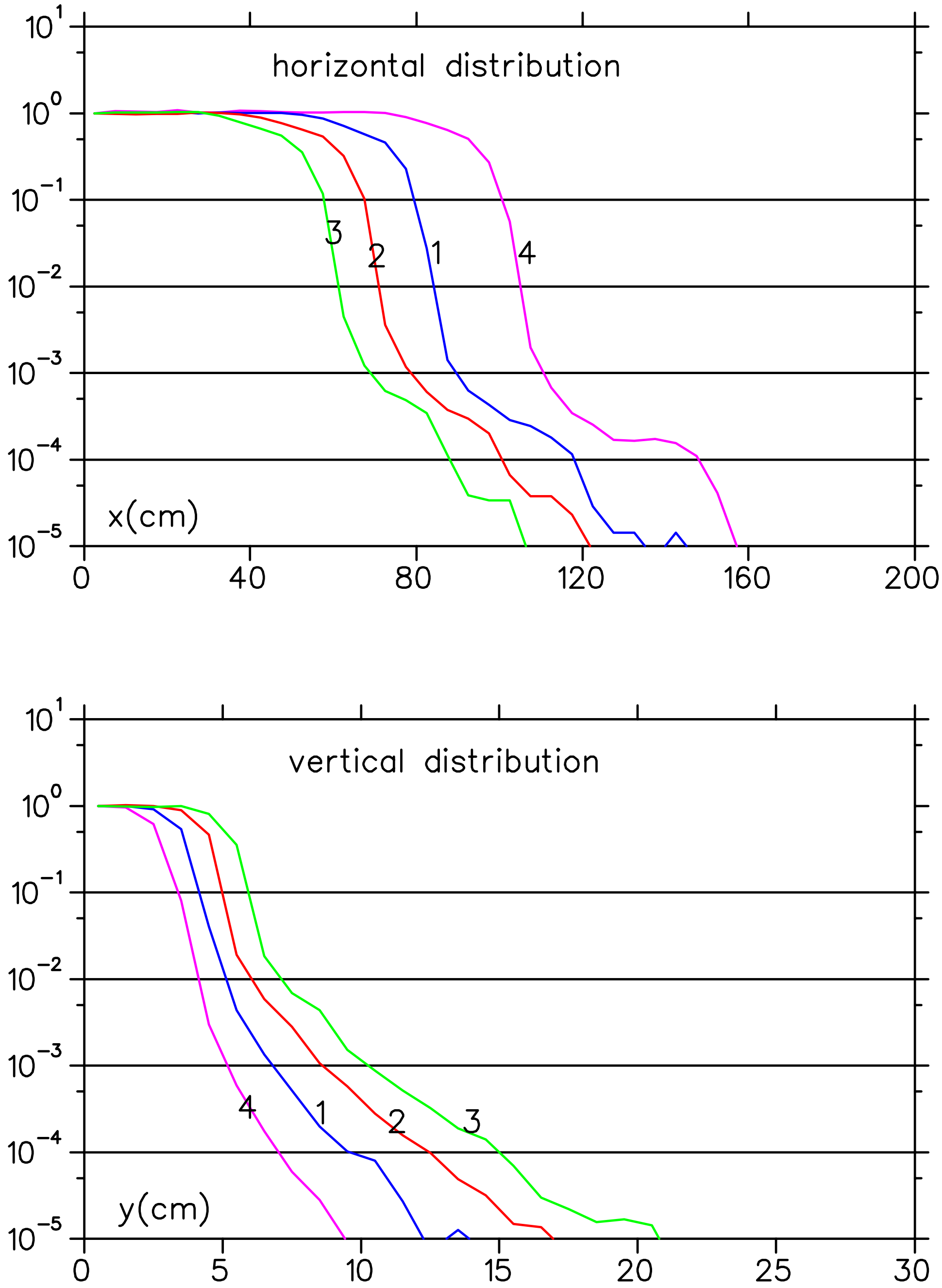

Figure 18: Normalized horizontal and vertical beam profiles at 14 m for all four cases

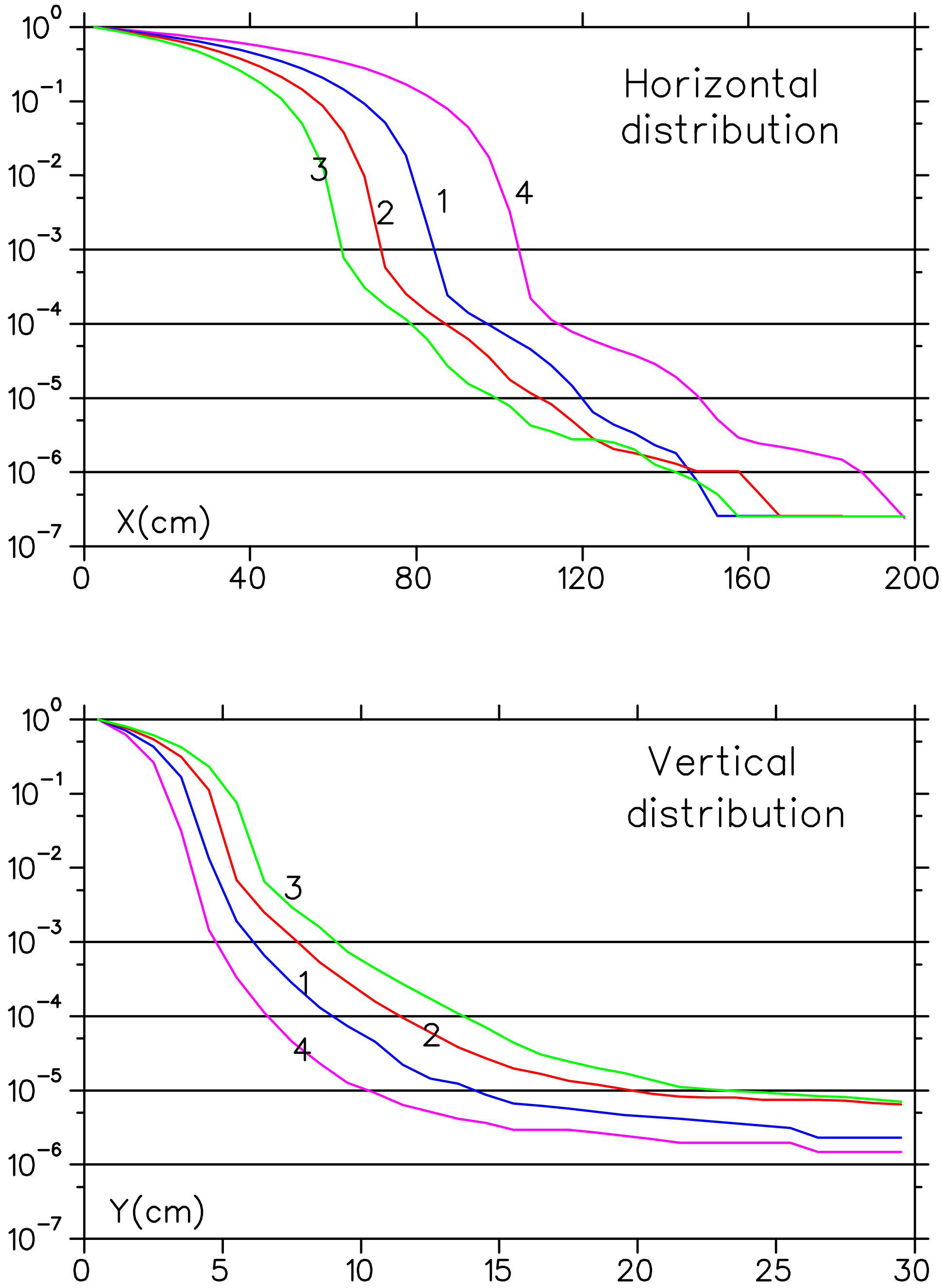

Figure 19: Fraction of beam outside the areas, indicated on the horizontal axis

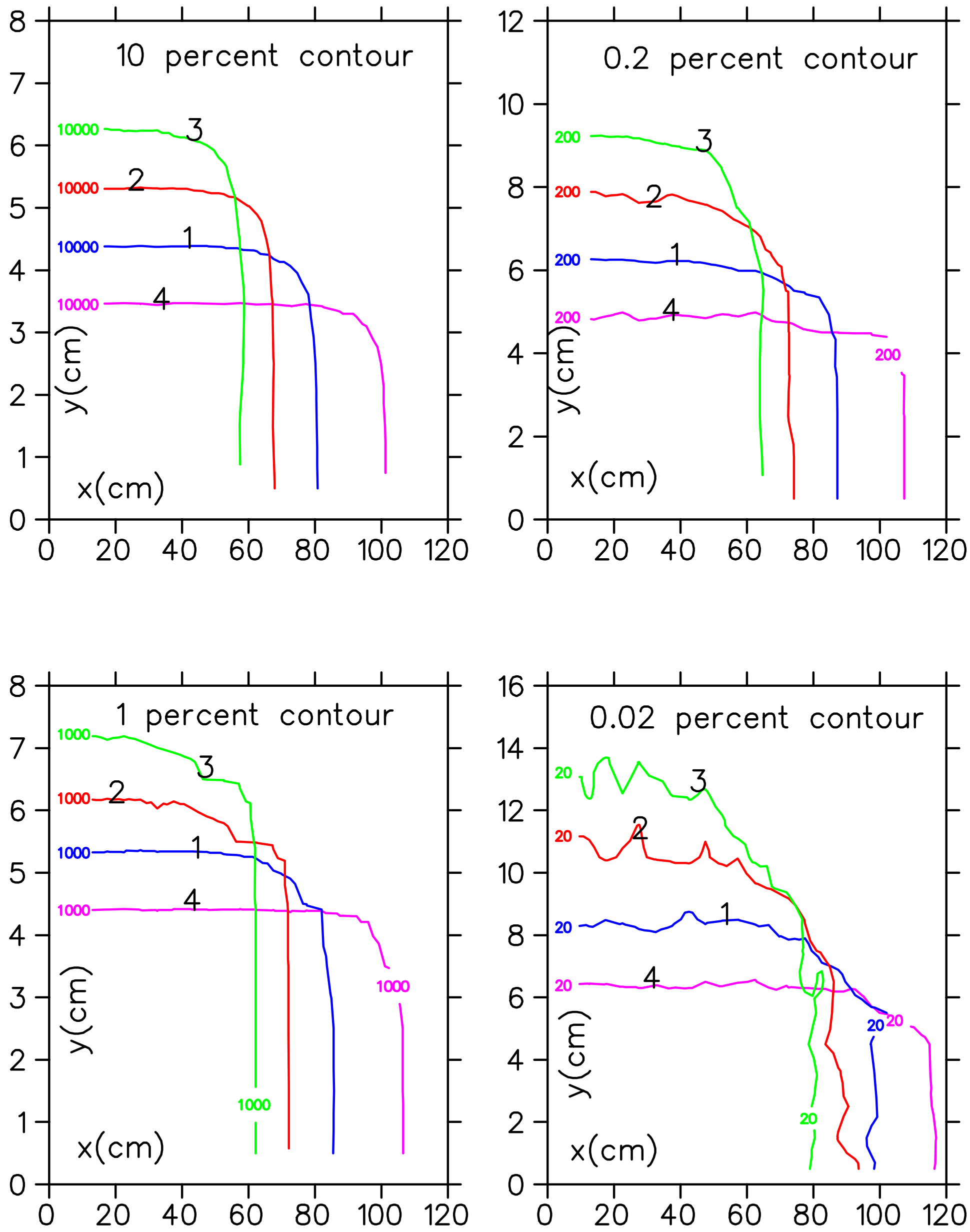

Figure 20: Contour plots at 14 m

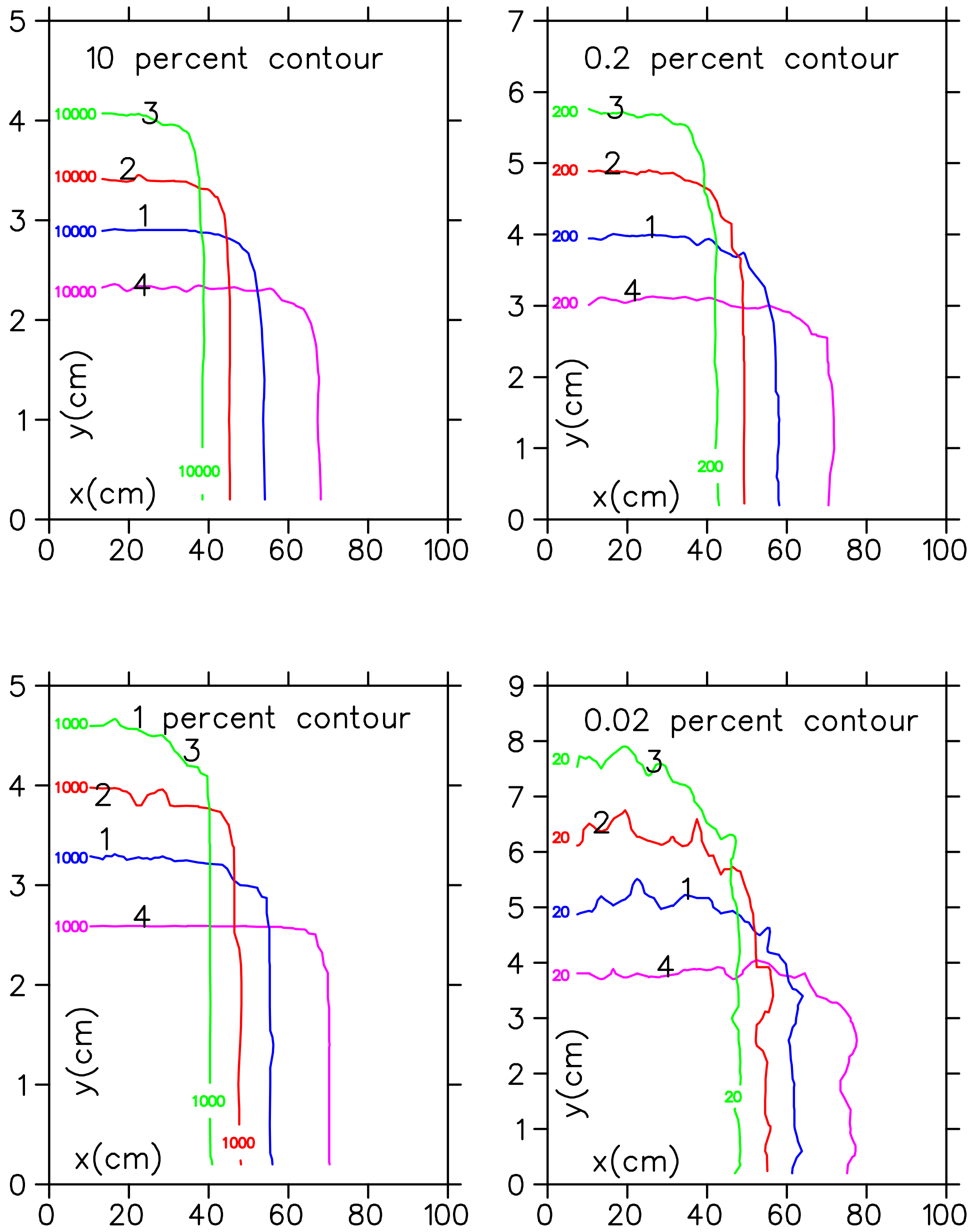

Figure 21: Contour plots at 9.5 m